

CONF-84C627--TC

UCRL- 90178
PREPRINT

Neutron Spectra as a Function of Angle
at Two Meters from the Little Boy Assembly

R. V. Griffith
C. J. Huntzinger
J. H. Thorngate

MASTER

Annual Health Physics Society Meeting
New Orleans, Louisiana
June 4-8, 1984

July 2, 1984

This is a preprint of a paper intended for publication in a journal or proceedings. Since changes may be made before publication, this preprint is made available with the understanding that it will not be cited or reproduced without the permission of the author.

 Lawrence
Livermore
Laboratory

NOTICE
PORTIONS OF THIS REPORT ARE ILLEGIBLE
It has been reproduced from the best
available copy to permit the broadest
possible availability.

DISTRIBUTION OF THIS DOCUMENT IS UNLIMITED

DISCLAIMER

This document was prepared as an account of work sponsored by an agency of the United States Government. Neither the United States Government nor the University of California nor any of their employees, makes any warranty, express or implied, or assumes any legal liability or responsibility for the accuracy, completeness, or usefulness of any information, apparatus, product, or process disclosed, or represents that its use would not infringe privately owned rights. Reference herein to any specific commercial products, process, or service by trade name, trademark, manufacturer, or otherwise, does not necessarily constitute or imply its endorsement, recommendation, or favoring by the United States Government or the University of California. The views and opinions of authors expressed herein do not necessarily state or reflect those of the United States Government thereof, and shall not be used for advertising or product endorsement purposes.

NEUTRON SPECTRA AS A FUNCTION OF ANGLE AT TWO METERS
FROM THE LITTLE ROY ASSEMBLY.*

UCRL--90178

R. V. Griffith, C. J. Huntzinger and J. H. Thorngate,

DE84 017033

Abstract

Measurements of neutron spectra produced by the Los Alamos National Laboratory (LANL) Little Roy replica assembly (Comet) were made with a combined multisphere and liquid scintillator system, that has been widely used at the Lawrence Livermore National Laboratory. The combined system was used for measurements at the side (90°) and nose (0°) of the assembly; additional measurements were made at 45° using only the liquid scintillator. Data were obtained at two meters from the center of the reactive region of the assembly, with good agreement between the multisphere and scintillator results. Comparison with liquid scintillator measurements performed by experimenters from the Canadian Defence Research Establishment, Ottawa (DREO) and calculations from LANL depended on the specific angle, obtaining the best agreement at 90° .

DISCLAIMER

This report was prepared as an account of work sponsored by an agency of the United States Government. Neither the United States Government nor any agency thereof, nor any of their employees, makes any warranty, express or implied, or assumes any legal liability or responsibility for the accuracy, completeness, or usefulness of any information, apparatus, product, or process disclosed, or represents that its use would not infringe privately owned rights. Reference herein to any specific commercial product, process, or service by trade name, trademark, manufacturer, or otherwise does not necessarily constitute or imply its endorsement, recommendation, or favoring by the United States Government or any agency thereof. The views and opinions of authors expressed herein do not necessarily state or reflect those of the United States Government or any agency thereof.

*This work was performed under the auspices of the U.S. Department of Energy by Lawrence Livermore National Laboratory under contract No. W-7405 ENG-48.

I. Introduction

Since a major portion of the understanding of radiation effects on humans depends on data from the Japanese bomb survivors, considerable effort has been expended to provide the necessary dosimetry. The recent availability of better source terms led to the recalculation of the dose-versus-distance relationships.¹ These calculations produced results at variance with the previously used T65D values,² particularly for Hiroshima. As a result, a critical assembly was constructed at LANL to mock up the Hiroshima weapon "Little Boy". The leakage radiation from this assembly has been measured by a number of groups. We made neutron spectrum measurements at three angles around the assembly, two meters from the center.

Our measurements used a multisphere system and a liquid scintillator system. In both cases, preliminary data reductions were done in the field. The scintillator, with careful data acquisition and reduction, can provide reasonably high resolution spectra over the energy range of 0.5 to 20 MeV, while the multisphere system can provide low-resolution data from 2.5×10^{-8} to 10 MeV. Therefore, the scintillator provides the bulk of the information above 1 MeV where the multisphere resolution is more limited, and the multisphere provides information in the energy region below the range of the scintillator, thus combining the data from the two systems.

II. Detectors

Liquid Organic Scintillator

Neutrons interact with an organic scintillator primarily by the production of recoil protons. The liquid organic scintillator NE-213 (Nuclear Enterprises Ltd., Edinburgh, Scotland) has gained wide acceptance for

measuring fast neutron spectra ($E_n > 100$ keV). A large part of its popularity is because protons and electrons produce light pulses with sufficiently different decay constants that the pulses can be electronically separated over a wide energy range. Liquid scintillators possess other advantages: They can be made in almost any desired shape and size, and their homogeneous nature eliminates the non-isotropic light production which occurs in solid organic scintillators.

The need to hold a liquid scintillator in some sort of a cell can be a problem for some applications. The detector used for these measurements had a cylindrical glass cell enclosing a liquid scintillator 5.08-cm in diameter by 5.08-cm high. The cell was designed for mounting in any orientation.

Liquid organic scintillators produce considerably less light for a given electron energy deposition than does a NaI scintillator; thus they have poorer resolution. Also, the light produced by protons in an organic scintillator is not a linear function of the energy deposited. For example, a 20-MeV proton produces about 200 times more light than a 0.5-MeV proton. To ensure that the relation between output current and incident light stays linear over this wide range of light values, the circuit providing the operating voltages for the photomultiplier tube must be designed to accommodate large surges in current and remain stable.³ The circuits used to amplify the signals must also be capable of handling this large dynamic range.

To differentiate between neutron- and gamma-ray-produced pulses, we use the pulse shape discriminator (PSD) described by Adams and White⁴ (commercially available as the Link System, Ltd. PSD 5010). This circuit is the best we found among the many techniques which have been reported. Even it, however, has pulse-rate and dynamic-range limitations which affect data

acquisition. Dynamic range limitations make it necessary to use two gain settings to cover the neutron energy range from 0.5 to 20 MeV. Our standard technique divides the measurements into one range from about 1.5 to 20 MeV and a second range from about 0.5 to 2 MeV. This provides an overlap to ensure that the runs are consistent.

Multispheres

The use of multisphere-moderated neutron spectrometry dates back more than 20 years.⁵ The advantages of this technique are simplicity of operation, increased sensitivity, and production of spectral information over the full neutron energy range. A major disadvantage is the limited energy resolution.

The multisphere system used at the Lawrence Livermore National Laboratory (LLNL) includes a 12.7 x 12.7 mm ⁶LiI crystal with polyethylene spheres 7.6, 12.7, 20.3, 25.4 and 30.5 cm in diameter. The 7.6 and 12.7 cm spheres are covered with 0.050-m thick cadmium shells to suppress thermal neutron response.

III. Data Acquisition

The detectors were mounted on a special handling device designed to allow measurements at angles from 90° (side) to 0° (nose) while maintaining a constant distance of 2 meters to the center of the assembly. We made our measurements during the week of April 25, 1983, when the Comet assembly was operated outside the containment building.

Organic Scintillator

Generally the low gain (1 - 20 MeV) data were taken first since the spectra had most of their information in this range. Before taking neutron data we performed pulse height calibrations using the Compton edges produced by the three gamma rays from ^{207}Bi (edges at 0.393, 0.858, 1.55 MeV), the two from ^{22}Na (0.341 and 1.07 MeV) and one from ^{137}Cs (0.482 MeV). Considerable extrapolation of the calibration data was required to cover the entire range of the measurement. A similar set of gamma ray data was taken after the neutron run. The gamma data were fit with a least square straight line using light values from our gamma-ray light yield measurements.⁶ This assumes that any gain drift occurred linearly during the course of the neutron run and that an average is the best representation of the adjustment which must be made.

For the high-gain runs (0.3 - 2 MeV), the 60 keV gamma ray from ^{241}Am and the Compton edges from the least energetic gamma rays of ^{22}Na and ^{207}Bi are used for pulse-height calibration. In this case, the ^{207}Bi gamma ray produces a calibration point nearly 60% of full scale, requiring less extrapolation and allowing a good calibration with fewer points.

Multispheres

The LiI detector is used with a portable pulse-height analyzer to provide immediate measurement of the detector responses. The main feature of the pulse-height spectrum is the peak due to the ^6LiI (n,α) reaction. The area of the n,α peak (after subtracting the continuum due to gamma background and other neutron interactions) is used as the detector response. We use a logarithmic interpolation between the minimum below the n,α peak and the point at which the n,α events appear to no longer contribute to

the spectrum. We have found that the 0.5 inch x 0.5 inch LiF crystal is sufficiently sensitive to measure spectra at a level of 1 nSv over a period of a few hours.

Spectrum determinations are usually made by leaving the crystal in a fixed position and taking individual measurements with the various spheres in position over the detector. In addition to the sphere measurements, we also take counts with and without a 0.05-cm-thick cadmium sleeve over the crystal. Measurements of the Comet Assembly were made at two meters using the special handling device. We measured only the 0° and 90° points with the multisphere system.

IV. Data Reduction

Organic Scintillator

The data reduction program used was based on the realization that the recoil-proton spectrum can be expressed as a convolution of the neutron spectrum and the recoil-proton cross section. The neutron spectrum can be deduced by differentiating the recoil-proton data. This ignores the distortions in the recoil-proton spectrum from nonlinear light output, edge effects, or multiple scattering. Data reduction programs using differentiation differ primarily in how they compensate for these distortions. The largest distortion is caused by the nonlinear light output. If these techniques are to work properly, the relation between scintillator light output and proton energy must be well-known. These data have been taken over varying energy ranges by a large number of workers, with considerable disagreement between their results. The carbon scattering, carbon reactions, multiple scattering- and edge-effect corrections vary

widely, and all involve approximations. Despite these limitations, neutron spectrum reduction using differentiation retains considerable popularity because it can be done on small, even portable, computer systems.⁷

Because the relation between proton energy and light output is so important, we made a large number of measurements with monoenergetic neutrons to verify this function for our detectors. As might be expected, our results are not in complete agreement with previous measurements. The response to gamma-ray sources is widely used as a means of providing a pulse-height calibration for these detectors, so we also made a number of careful measurements to determine light output as a function of electron energy.

Our data-reduction program starts by rebinning the data in 0.1 MeV increments of proton energy. An advantage of this procedure is that the results are always given in the same, uniform energy groups. This is particularly convenient when combining data measured at different gains or from multiple runs. The corrections we presently use for efficiency, multiple scattering, and edge effects are the same as those used by Slaughter in NUTSPEC,⁸ most of which were accumulated from various sources by Toms.⁹ After rebinning, the data are differentiated in the simplest possible way, using differences of adjacent energy bins. Johnson has pointed out that other differentiation procedures can result in distortions of the data.¹⁰

After differentiation, the data are smoothed with a Gaussian function whose width varies in a manner similar to the change of resolution of the detector as a function of light output. The relation between light and resolution is of the form reported by Dietze with the constants derived from the Compton recoil electron data.¹¹

The data-reduction program is used with a small computer (Hewlett-Packard HP-85) which can easily be taken into the field. A second program is used to transfer data directly from a portable multi-channel analyzer to this computer.

Multispheres

Accurate response functions are a vital aspect of the use of multispheres for spectrometry. Lack of monenergetic neutrons below 2 keV means that calculations must be used to produce a full energy response matrix. Calculations have been made for a large number of detector types over a range of sphere sizes.¹²⁻¹⁵ For some time we have used response functions based on the calculations by Sanna,¹⁵ which recognize that the polyethylene used for spheres ranges in density from 0.9 to 1.0 g/cm³. These calculations also provide data for interpolation using actual CH₂ densities. For the smaller spheres this effect is not serious, but at diameters of 25 cm or more the result could be in error of as much as 40 to 100% in the expected thermal neutron response.

The last basic requirement is a mathematical method for unfolding the spectrum from the response matrix. A number of computer codes have been developed to attack this class of unfolding problem.¹⁶⁻²⁶ For a number of years, we have used the Fortran LOUHI code developed at the Lawrence Berkeley Laboratory.^{17,24} LOUHI is designed to obtain the solution of Fredholm integral equations of the first kind by using a generalized least-squares procedure with non-negative solution.

With LOUHI, any given energy bin can be "TIED" to a specific fluence value if the experimenter has independent knowledge of that value. Therefore,

we can use spectral data from high-resolution spectrometry systems, such as the organic scintillator, to establish the higher-energy portion of the spectrum in order to evaluate the low and intermediate bins more effectively. The result is a hybrid spectrum with potentially improved accuracy.

We have recently begun using the SPUNF code developed for desk top computers (Hewlett-Packard 85).²² This code provides us with true portability previously lacking in our multispher system. Although the code does not have some of the features of LOUHI (for example, the result is dependent on the trial solutions), the results are quite comparable. This is particularly true when comparing spectrum-averaged values from each, such as the quality factor, dose equivalent rate, and average neutron energy.

Results

The results of our measurements are presented in Tables 1-3 and Figs. 1-3. The first figures show multispher results at 0° and 90°. Fewer neutrons and a somewhat softer spectrum were obtained at 0° than at 90°. The liquid scintillator results shown in Fig. 2 confirm this with the 45° data falling between the 0° and 90° data. When the data from the two systems are combined for the 0° and 90° cases, the results shown in Fig. 3 are obtained. The effect of considering the scintillator results while processing the multispher data is small. This confirms that the data from the two systems are consistent.

For purposes of comparison, experimenters from the Defence Research Establishment, Ottawa (DREO) have made measurements using an NE-213 fast-neutron spectrometer at seven polar angles from 0 to 135 degrees and distances

of 75 and 200 cm from the center of the Comet assembly.²⁷ Those measurements were made inside a containment building which contributed additional background components not present in our measurements. The DREO experimenters did, however, take steps to compensate for the building background except at 0°. In addition to these measurements, neutron transport calculations have been made at LANL.²⁸ A recent, unpublished set of calculations with improved statistical precision²⁹ has been used for comparison. These calculations do not include scattering from the ground or building materials.

Comparisons of the LLNL measurements and LANL calculations over the range 10^{-7} to 10 MeV are presented in Figs. 4 and 5. The lack of scatter contribution is evident in the spectral difference below about 100 eV. The 25-keV peak due to transmission through the steel assembly case is present in the calculated spectra, but not found in the LLNL composite spectrum because of the poor multisphere resolution.

Figures 6-11 show the comparison of the calculated spectra with the two measurements. The agreement at 0° is clearly poor. The neutron intensity is lowest at this angle, so that background related errors could cause serious differences. Neither LLNL nor DREO made background corrections at 0°. The DREO measurements were made in the containment building with other neutron sources present, while the LLNL measurements were made outside. As the angle increases through 45° to 90° the agreement between both measurement sets and calculations improves dramatically.

Spectrum-weighted values of kerma,³⁰ dose equivalent,³¹ and absorbed dose (Element 57 of the Snyder phantom³²) have also been calculated from these data (Table 4). The full energy range weightings show significant differences, primarily the result of the differences in the values of fluence per

fission. Moreover, differences in spectral shape at low energies result in different fluence-to-dose (equivalent) conversion factors. These differences add to the overall disparity. The weighted dosimetric parameters in the range 1 to 10 MeV again show the large disagreement at 0°, narrowing to $\pm 20\%$ at 45° and $\pm 9.8\%$ at 90°.

References

1. Loewe, W. E. and Mendelsohn, E., "Revised Dose Estimates at Hiroshima and Nagasaki," Hlth. Phys. 41 (663-666), 1981.
2. Auxier, J. A., "Ichiban: Radiation Dosimetry for the Survivors of the Bombings of Hiroshima and Nagasaki," Technical Information Center, ERDA, Oak Ridge, TN, TID-27080.
3. Reiter, W. L. and Stengl, G. "Two Types of Photomultiplier Voltage Dividers for High and Changing Count Rates," Nucl. Instr. and Meth. 174 (585-591) 1980.
4. Adams, J. M. and White, G. "A Versatile Pulse Shape Discriminator for Charged Particle Separation and Its Application to Fast Neutron Time-of-Flight Spectroscopy," Nucl. Instr. and Meth. 156 (459-476) 1978.
5. Bramblett, R. L., Ewing, R. J., and Bonner, T. W. "A New Type of Neutron Spectrometer," Nucl. Inst. Meth., Vol. 9, 1-12 (1960).
6. Thorngate, J. H., and Rueppel, D. W. "Neutron Spectrometry Developments: Detector Improvements and Characterization," in Hazards Control Department Annual Technology Review 1981, Lawrence Livermore National Laboratory, Livermore, CA, UCRL-50007-81 (1982).
7. Hunt, G. F., Kaifer, R. C., Slaughter, D. R., Strout II, R. E. and Rueppel, D. W. "A Microprocessor-Controlled Portable Neutron Spectrometer," IEEE Trans. Nuc. Sci. NS-27 (757-763) 1980.

8. Slaughter, D. R. "Nutspec: A Program for Unfolding Neutron Spectral Data Obtained with Scintillation Detectors and Gas Proportional Counters," Lawrence Livermore Laboratory, Livermore, CA, UCID-17713 (1978).
9. Toms, M. E. "A Computer Analysis to Obtain Neutron Spectra from an Organic Scintillater," Nucl. Instr. and Meth. 92 (61-70) 1971.
10. Johnson, R. H. "Improvements in the Differentiation Method of Spectrum Unfolding," Nucl. Instr. and Meth. 179 (301-307) 1981.
11. Dietze, G. "Energy Calibration of NE-213 Scintillation Counters by τ -Rays," IEEE Trans. Nucl. Sci. NS-26 (398-402) 1979.
12. Caizergues, R. and Poullot, G. Calcul De La Response Des Spheres De Bonner Pour Les Detecteurs Li, He et Mn - Comparaison Avec Les Donnees Experimentales Pour L'iodure De Lithium, Commissariat L'Energies Atomique, Centre d'Etudes Nucleaires de Saclay, Rappart CEA-R-4400 (1972).
13. Mourguès, M. "La Measure des Neutrons par Computer a Helium-3 Sous Moderateur Spherique," Proc. Second Symposium on Neutron Dosimetry in Biology and Mediciane, 907-928, Commission of the European Communities Rept. EUR 5273 d-e-f (1975).
14. Nachtigall, D. and Burger, G. "Dose Equivalent Determinations in Neutron Fields by Means of Moderator Techniques," Topics in Radiation Dosimetry, Supplement 1 to Radiation Dosimetry, F. H. Attix, Ed. (Academic Press, New York, 1972) pp. 385-459.
15. Sanna, R. S. Thirty One Group Response Matrices for the Multisphere Neutron Spectrometer Over the Energy Range Thermal to 400 MeV, U.S.A.E.C. Health and Safety Laboratory Rept., HASL-267 (1973).
16. Jacobs, G. J. H. and van den Bosch, R. L. P. "Calibration Measurements with the Multisphere Method and Neutron Spectrum Analyses Using the SAND-II Program," Nuc. Inst. and Meth., 175, (483-489) (1980).

17. Routti, J. T. "Mathematical Considerations of Determining Neutron Spectra from Activation Measurements," Proc. Second Intern. Symp. on Accelerator Dosimetry and Experience, Stanford University, 1969, CONF-691101.
18. Zijp, W. L. "Comparison of Neutron Spectrum Unfolding Codes," Neutron Cross Sections for Reactor Dosimetry, IAEA-208, Vol. II, 37-62 (1978).
19. Sanna, R. S. "Modification of an Iterative Code for Unfolding Neutron Spectra from Multisphere Data," U.S. ERDA Report HASL-311 (October, 1976).
20. McElroy W. N., Berg, S., and Crockett, T. "A Computer-Automated Iterative Method for Neutron Flux Spectra Determination by Foil Activation," Air Force Weapons Laboratory Rept. AFWL-TR-67-41, Vol. I and II (1967).
21. Zaidins, C.S., Martin, J. B., and Edwards, F. M. "A Least-Squares Technique for Extracting Neutron Spectra from Bonner Sphere Data," Med Phys, 5(1):42-47 (1978).
22. Hajnal, F. An Iterative Nonlinear Unfolding Code: TWOGO, USDOE Report EML-391 (1981).
23. Hajnal, F. Private Communication (1982).
24. Routti, J. T. and Sanberg, J. V. General Purpose Unfolding Program LOUHI 78 with Linear and Nonlinear Regularizations, Helsinki University of Technology Report TkK-F-A359 (1978).
25. Sanna, R. S. A Manual for BON: A Code for Unfolding Multisphere Spectrometer Neutron Measurements, DOE Environmental Measurements Laboratory Rept. EML-394 (1981).
26. O'Brien, K. and Sanna, R. S. "Neutron Spectral Unfolding Using the Monte Carlo Method," Nuc. Inst. and Meth. 185, 277-281 (1981).

27. Robitaille, H. A. and Haffarth, R. E., Neutron Leakage from "Comet" - A Duplicate Little-Boy Device, Department of National Defence, Canada, Defence Research Establishment Ottawa, DREO Report R-878 (July 1983).
28. Whalen, P. P., Soran, P. D., Malenfant, R., and Forehand, H. M., Jr., "Experiments at Los Alamos National Laboratory with the Replica of the Hiroshima Weapon," Proceedings of the Second U.S.-Japan Joint Workshop for Reassessment of Atomic Bomb Radiation Dosimetry in Hiroshima and Nagasaki, pp. 21-25 (November 1983).
29. Hendricks, J. S. and Whalen, P. P., Unpublished (1984).
30. International Commission on Radiation Units and Measurements. Neutron Fluence, Neutron Spectra and Kerma, ICRU Publications, Washington DC, ICRU Report 13 (1969).
31. International Committee on Radiation Protection. Data for Protection Against Ionizing Radiation from External Sources: Supplement to ICRP Publication 15. Publication 21, Pergamon Press, Oxford (1971).
32. Auxier, J. A., Snyder, W. A and Jones, T. D., "Neutron Interactions and Penetration in Tissue," Radiation Dosimetry, Volume I-Fundamentals, Attix, F. H. and Roesch, W. C., Eds. (Academic Press, New York, 1968) pp. 275-316. (1968).

Table 1

Composite Little Boy Replica Neutron Spectrum
2 meters - 0°

Lower Energy Bound (MeV)	Fluence ($n \cdot \text{cm}^{-2} \text{ MeV}^{-1} \cdot \text{Fission}^{-1}$)	Lower Energy Bound (MeV)	Fluence ($n \cdot \text{cm}^{-2} \text{ MeV}^{-1} \cdot \text{Fission}^{-1}$)
2.50×10^{-8}	$3.23 \pm 0.960 \times 10^{-2}$	0.95	2.29 ± 0.067
4.14×10^{-7}	1.45 ± 0.676	1.05	1.39 ± 0.045
6.83	$6.41 \pm 3.48 \times 10^{-3}$	1.15	$8.10 \pm 0.276 \times 10^{-9}$
1.44×10^{-6}	2.77 ± 1.38	1.25	5.29 ± 0.214
3.06	1.17 ± 0.57	1.35	3.33 ± 0.176
6.48	$4.93 \pm 3.05 \times 10^{-4}$	1.45	2.63 ± 0.157
1.37×10^{-5}	2.10 ± 1.64	1.55	2.39 ± 0.136
2.90	$9.22 \pm 8.21 \times 10^{-5}$	1.65	2.02 ± 0.116
6.14	4.26 ± 4.03	1.75	1.53 ± 0.104
1.30×10^{-4}	2.10 ± 2.03	1.85	$9.43 \pm 1.03 \times 10^{-10}$
2.75	1.12 ± 1.08	1.95	7.65 ± 0.930
5.93	$6.53 \pm 6.12 \times 10^{-6}$	2.05	6.36 ± 0.928
1.23×10^{-3}	4.19 ± 3.70	2.15	5.43 ± 0.886
2.61	2.96 ± 2.35	2.25	4.66 ± 0.789
5.53	2.28 ± 1.54	2.35	3.85 ± 0.697
1.17×10^{-2}	1.88 ± 1.03	2.45	3.14 ± 0.643
2.48	1.62 ± 0.711	2.55	2.66 ± 0.612
5.25	1.36 ± 0.463	2.65	2.33 ± 0.595
0.111	1.01 ± 0.243	2.75	2.01 ± 0.587
0.224	$5.59 \pm 1.10 \times 10^{-7}$	2.85	1.63 ± 0.581
0.45	3.10 ± 0.098	2.95	1.30 ± 0.573
0.55	2.26 ± 0.068	3.05	1.21 ± 0.583
0.65	1.54 ± 0.047	3.15	1.40 ± 0.597
0.75	$8.29 \pm 0.245 \times 10^{-8}$	3.25	1.60 ± 0.588
0.85	4.10 ± 0.110	3.35	1.56 ± 0.553
		3.45	1.21 ± 0.510
		3.55	$7.36 \pm 4.85 \times 10^{-11}$
		3.65	3.84 ± 4.88
		3.75	2.67 ± 5.00
		3.85	3.23 ± 5.05
		3.95	4.46 ± 5.00
		4.05	

• Error estimates

2.50×10^{-8} to 0.45 MeV - Uncertainty of multisphere unfolding process
above 0.45 MeV - Statistical errors and cross section uncertainties
associated with NE-213 unfolding

Table 2
NE-213 Measured Little Boy Replica Spectrum
2 meters - 45°

Lower Energy Bound (MeV)	Fluence (n · cm ⁻² MeV ⁻¹ · Fission ⁻¹)	Lower Energy Bound (MeV)	Fluence (n · cm ⁻² MeV ⁻¹ · Fission ⁻¹)
0.45	7.06 ± 0.266 × 10 ⁻⁷	2.95	1.19 ± 0.202
0.55	6.00 ± 0.189	3.05	1.07 ± 0.195
0.65	4.44 ± 0.139	3.15	9.84 ± 1.89 × 10 ⁻¹⁰
0.75	2.54 ± 0.074	3.25	8.82 ± 1.81
0.85	1.36 ± 0.036	3.35	8.01 ± 1.75
0.95	8.04 ± 0.217 × 10 ⁻⁸	3.45	7.76 ± 1.71
1.05	5.15 ± 0.141	3.55	7.63 ± 1.67
1.15	3.44 ± 0.095	3.65	6.92 ± 1.60
1.25	2.41 ± 0.071	3.75	5.68 ± 1.54
1.35	1.62 ± 0.053	3.85	4.50 ± 1.48
1.45	1.17 ± 0.043	3.95	3.81 ± 1.45
1.55	1.03 ± 0.040	4.05	3.59 ± 1.43
1.65	9.10 ± 0.364 × 10 ⁻⁹	4.15	3.64 ± 1.41
1.75	7.28 ± 0.331	4.25	3.79 ± 1.38
1.85	5.72 ± 0.312	4.35	3.89 ± 1.34
1.95	5.26 ± 0.401	4.45	3.84 ± 1.29
2.05	4.46 ± 0.359	4.55	3.55 ± 1.23
2.15	3.73 ± 0.347	4.65	3.08 ± 1.19
2.25	3.08 ± 0.346	4.75	2.57 ± 1.15
2.35	2.57 ± 0.344	4.85	2.13 ± 1.13
2.45	2.24 ± 0.321	4.95	1.84 ± 1.11
2.55	2.01 ± 0.280	5.05	1.74 ± 1.11
2.65	1.82 ± 0.248	5.15	1.77 ± 1.10
2.75	1.62 ± 0.230	5.25	1.87 ± 1.09
2.85	1.39 ± 0.215	5.35	1.94 ± 1.07
		5.45	1.95 ± 1.04
		5.55	1.94 ± 1.00
		5.65	1.88 ± 0.970
		5.75	1.73 ± 0.934
		5.85	1.50 ± 0.906
		5.95	1.24 ± 0.889
		6.05	

Table 3

Composite Little Boy Replica Neutron Spectrum
2 meters - 90°

Lower Energy Bound (MeV)	Fluence (n · cm ⁻² MeV ⁻¹ · Fission ⁻¹)	Lower Energy Bound (MeV)	Fluence (n · cm ⁻² MeV ⁻¹ · Fission ⁻¹)
2.50 x 10 ⁻⁸	3.59 ± 1.59 x 10 ⁻²	0.95	1.70 ± 0.032
4.14 x 10 ⁻⁷	2.00 ± 0.930	1.05	1.17 ± 0.022
6.83	1.08 ± 0.561	1.15	8.09 ± 0.153 x 10 ⁻⁸
1.44 x 10 ⁻⁶	5.54 ± 2.69 x 10 ⁻³	1.25	5.81 ± 0.114
3.06	2.68 ± 1.16	1.35	4.02 ± 0.087
6.43	1.24 ± 0.601	1.45	2.71 ± 0.070
1.37 x 10 ⁻⁵	5.58 ± 3.48 x 10 ⁻⁴	1.55	2.45 ± 0.072
2.90	2.50 ± 1.87	1.65	2.61 ± 0.078
6.14	1.15 ± 0.954	1.75	2.38 ± 0.067
1.30 x 10 ⁻⁴	5.56 ± 4.48 x 10 ⁻⁵	1.85	1.92 ± 0.054
2.75	2.90 ± 2.54	1.95	1.37 ± 0.016
5.93	1.66 ± 1.42	2.05	1.17 ± 0.074
1.23 x 10 ⁻³	1.06 ± 0.854	2.15	9.87 ± 0.725 x 10 ⁻⁹
2.61	7.61 ± 5.48 x 10 ⁻⁶	2.25	8.44 ± 0.666
5.53	6.11 ± 3.70	2.35	4.34 ± 0.574
1.17 x 10 ⁻²	5.42 ± 2.59	2.45	6.43 ± 0.485
2.48	5.11 ± 1.83	2.55	5.67 ± 0.432
5.25	4.77 ± 1.27	2.65	5.07 ± 0.399
0.111	3.87 ± 0.743	2.75	4.59 ± 0.374
0.224	2.22 ± 0.353	2.85	4.15 ± 0.352
0.45	9.57 ± 0.216 x 10 ⁻⁷	2.95	3.73 ± 0.328
0.55	9.30 ± 0.200	3.05	3.35 ± 0.310
0.65	7.38 ± 0.160	3.15	3.08 ± 0.295
0.75	4.51 ± 0.091	3.25	2.87 ± 0.283
0.85	2.63 ± 0.048	3.35	2.62 ± 0.274

Table 3 (continued)

Composite Little Boy Replica Neutron Spectrum
2 meters - 90°

Lower Energy Bound (MeV)	Fluence ($n \cdot \text{cm}^{-2} \text{ MeV}^{-1} \cdot \text{Fission}^{-1}$)	Lower Energy Bound (MeV)	Fluence ($n \cdot \text{cm}^{-2} \text{ MeV}^{-1} \cdot \text{Fission}^{-1}$)
3.45	2.33 \pm 0.266	5.95	4.92 \pm 1.22
3.55	2.06 \pm 0.255	6.05	4.62 \pm 1.20
3.65	1.87 \pm 0.244	6.15	4.35 \pm 1.18
3.75	1.76 \pm 0.235	6.25	4.09 \pm 1.16
3.85	1.68 \pm 0.228	6.35	3.80 \pm 1.12
3.95	1.59 \pm 0.220	6.45	3.53 \pm 1.09
4.05	1.50 \pm 0.210	6.55	3.33 \pm 1.06
4.15	1.40 \pm 0.202	6.65	3.24 \pm 1.03
4.25	1.32 \pm 0.198	6.75	3.20 \pm 1.00
4.35	1.25 \pm 0.194	6.85	3.13 \pm 0.979
4.45	1.20 \pm 0.187	6.95	2.97 \pm 0.957
4.55	1.16 \pm 0.178	7.05	2.74 \pm 0.942
4.65	1.08 \pm 0.169	7.15	2.49 \pm 0.935
4.75	9.94 \pm 1.64 $\times 10^{-10}$	7.25	2.28 \pm 0.935
4.85	9.16 \pm 1.59	7.35	2.14 \pm 0.937
4.95	8.68 \pm 1.56	7.45	2.06 \pm 0.937
5.05	8.40 \pm 1.52	7.55	2.02 \pm 0.931
5.15	8.09 \pm 1.49	7.65	1.98 \pm 0.917
5.25	7.61 \pm 1.46	7.75	1.91 \pm 0.894
5.35	7.02 \pm 1.42	7.85	1.77 \pm 0.869
5.45	6.46 \pm 1.37	7.95	1.61 \pm 0.846
5.55	6.05 \pm 1.34	8.05	
5.65	5.76 \pm 1.31		
5.75	5.50 \pm 1.28		
5.85	5.23 \pm 1.25		

Table 4
Spectrum Weighted Dosimetric Quantities

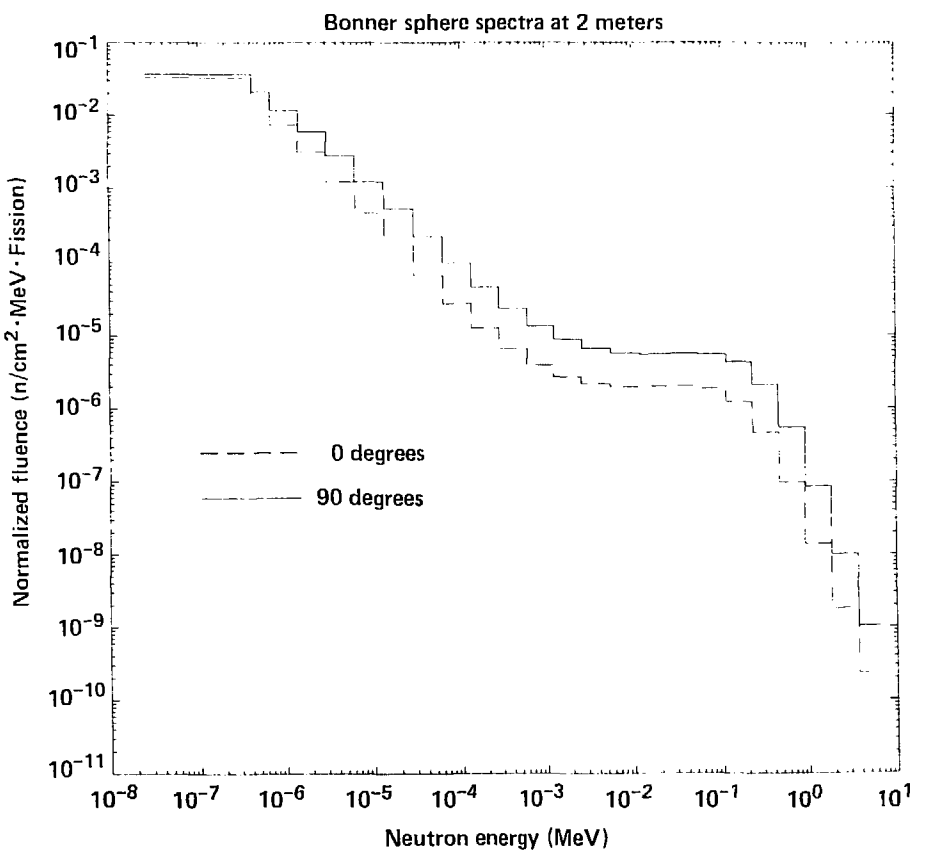
$4.14 \cdot 10^{-7}$ to 1- MeV

		<u>KERMA</u>	<u>ICRPDE</u>	<u>EL57</u>
<u>0°</u>	n/cm ² • Fission	Ergs/gm/fission	Rem/Fission	Rad/Fission
LLNL	$5.47 \cdot 10^{-7}$	$0.497 \cdot 10^{-13}$	$5.64 \cdot 10^{-15}$	$0.638 \cdot 10^{-15}$

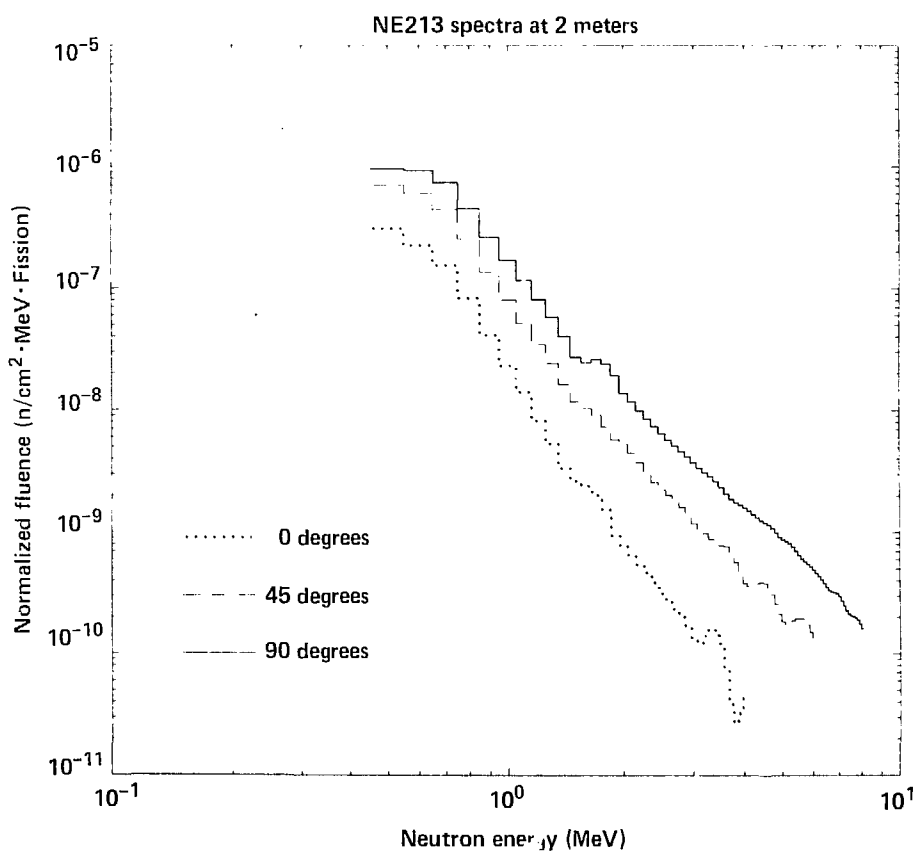
<u>90°</u>				
LLNL	20.0	2.08	24.0	2.62
LANL	16.1	1.36	15.6	1.82

1.0 to 10 MeV

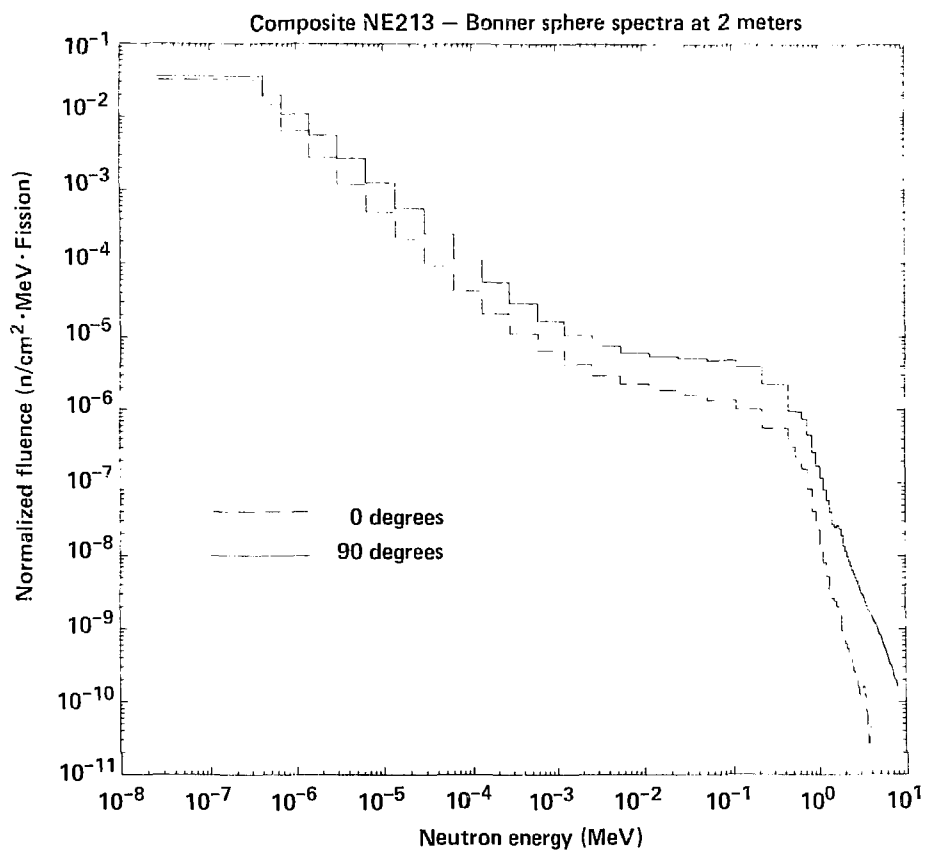
<u>0°</u>				
LLNL	$0.0566 \cdot 10^{-7}$	$0.0146 \cdot 10^{-13}$	$0.198 \cdot 10^{-15}$	0.0186
LANL	0.0327	0.00840	0.114	0.0107
DREO	0.139	0.0392	0.505	0.0498
<u>45°</u>				
LLNL	0.252	0.0670	0.879	0.0852
LANL	0.204	0.0542	0.724	0.0691
DREO	0.299	0.0813	1.08	0.104
<u>90°</u>				
LLNL	0.630	0.176	2.27	0.224
LANL	0.565	0.155	2.03	0.196
DREO	0.683	0.188	2.47	0.238



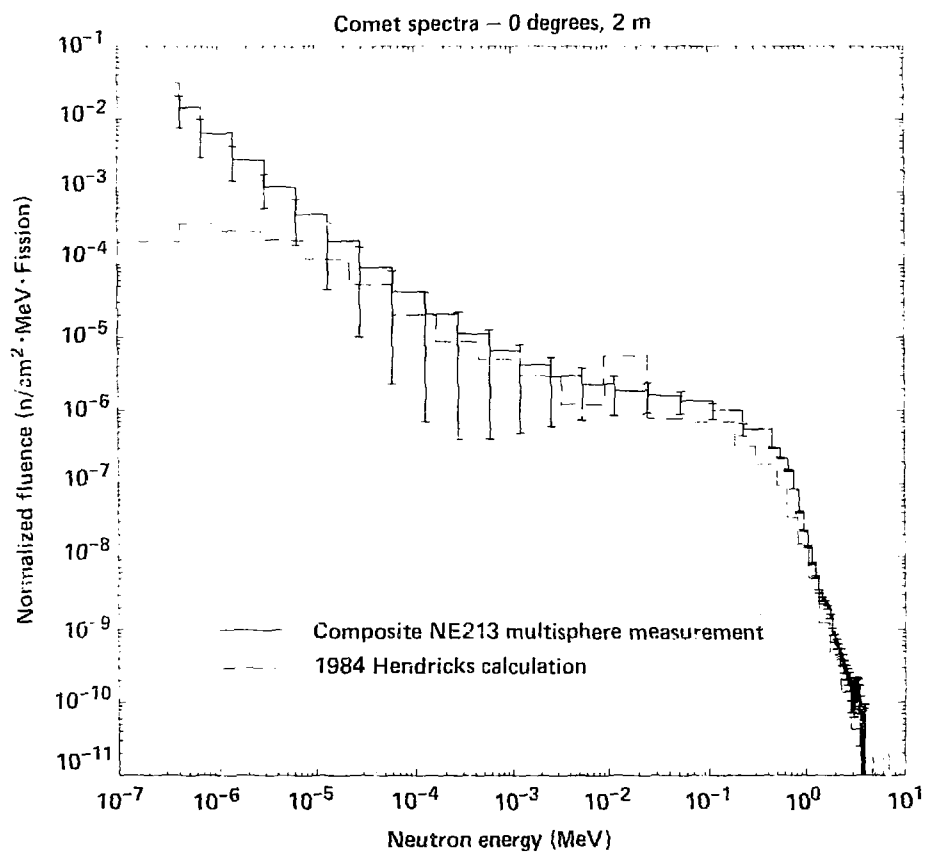
Griffith - Fig. 1



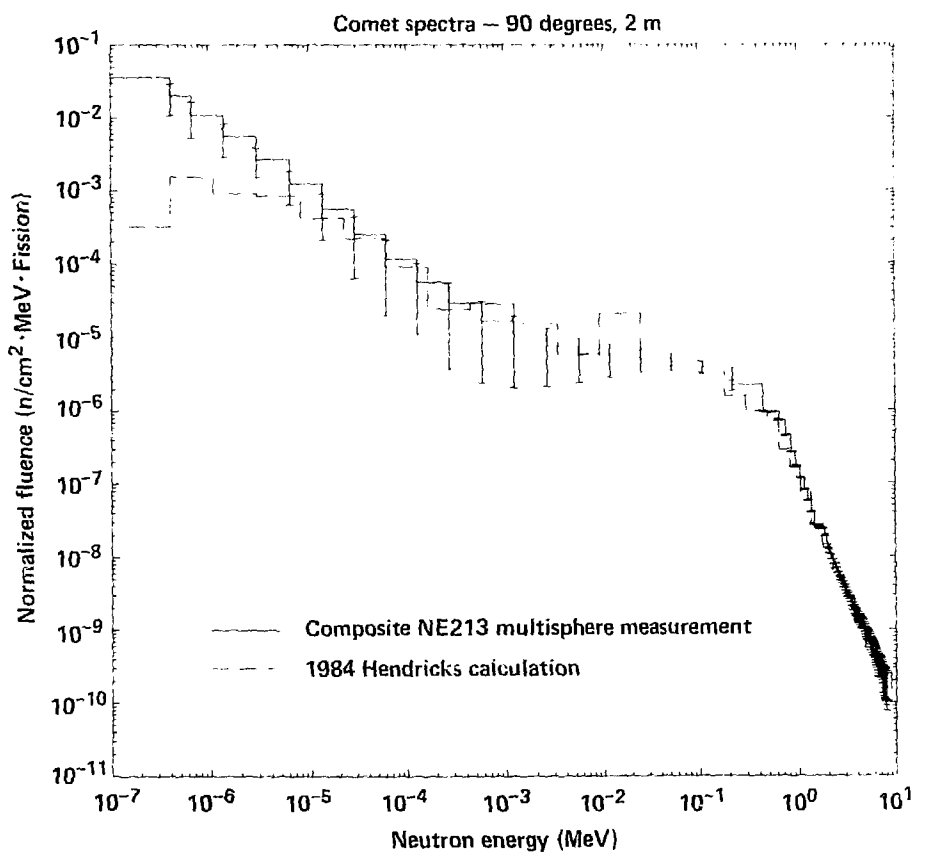
Griffith - Fig. 2



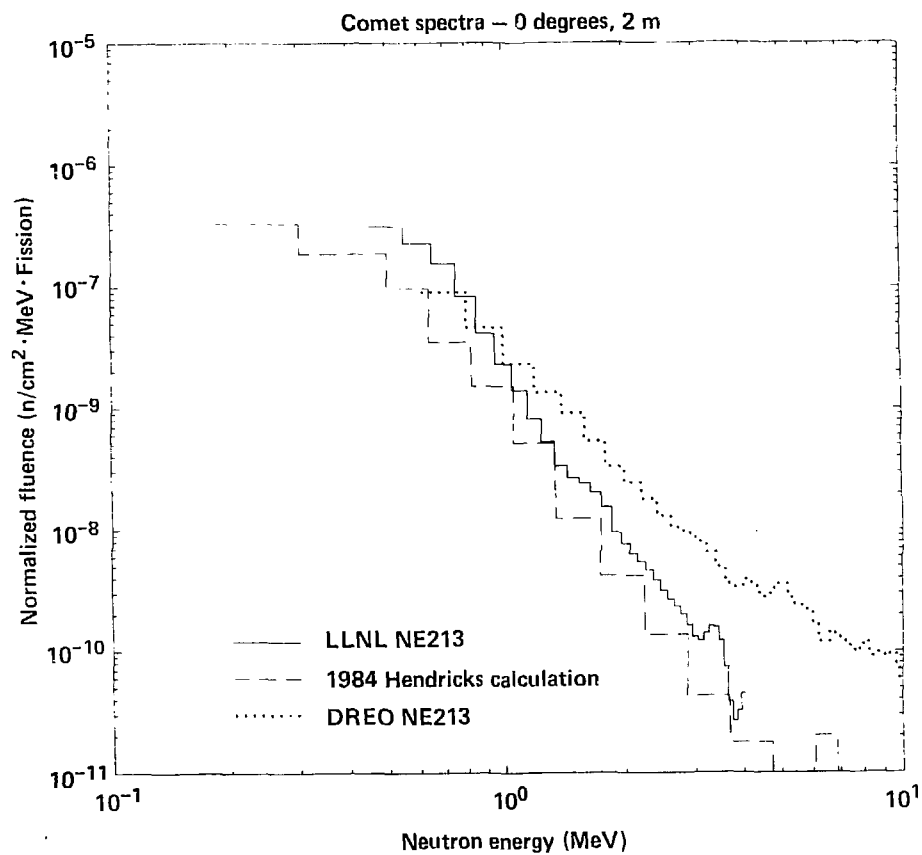
Griffith - Fig. 3



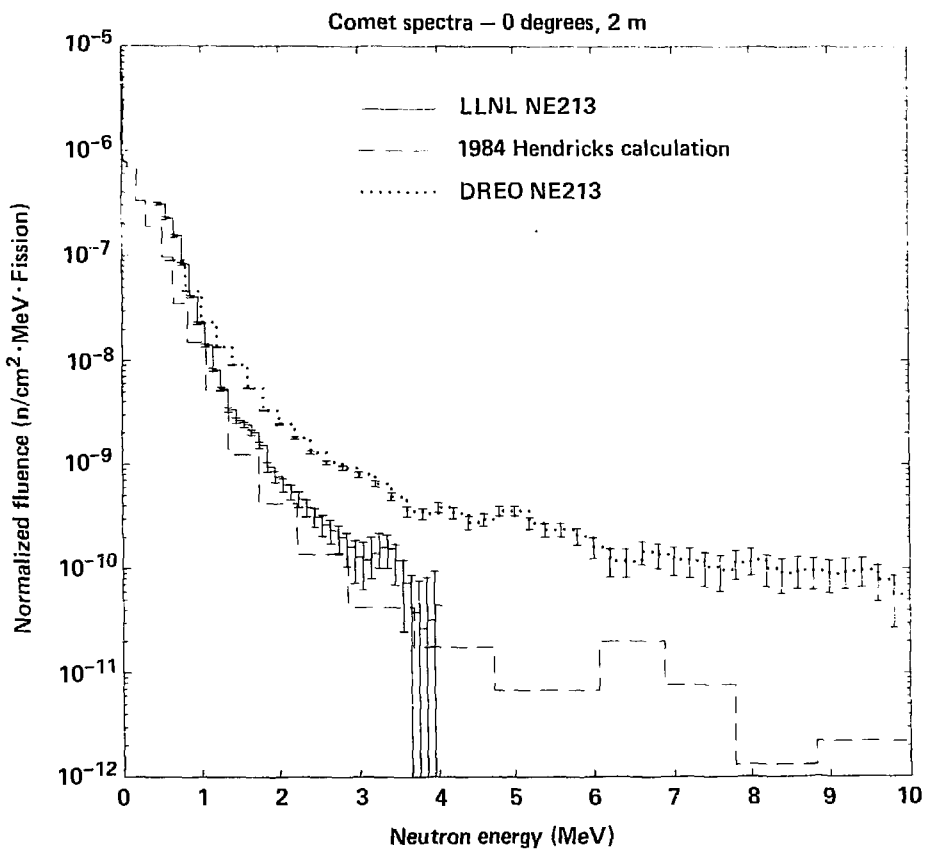
Griffith - Fig. 4



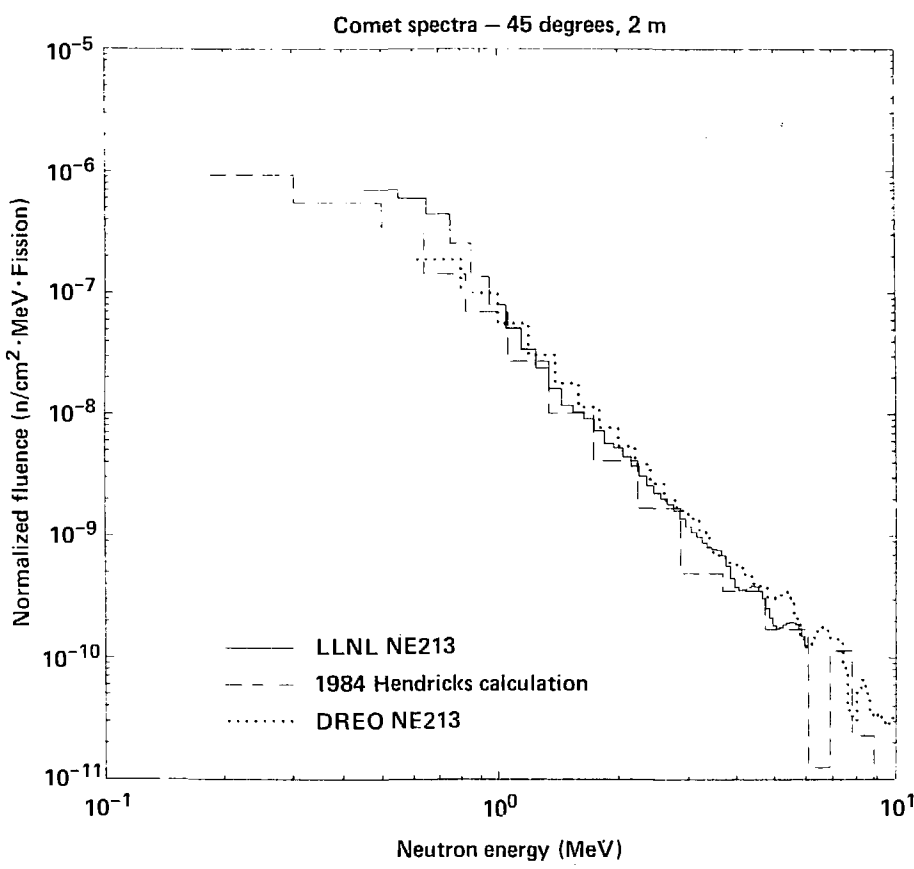
Griffith - Fig. 5



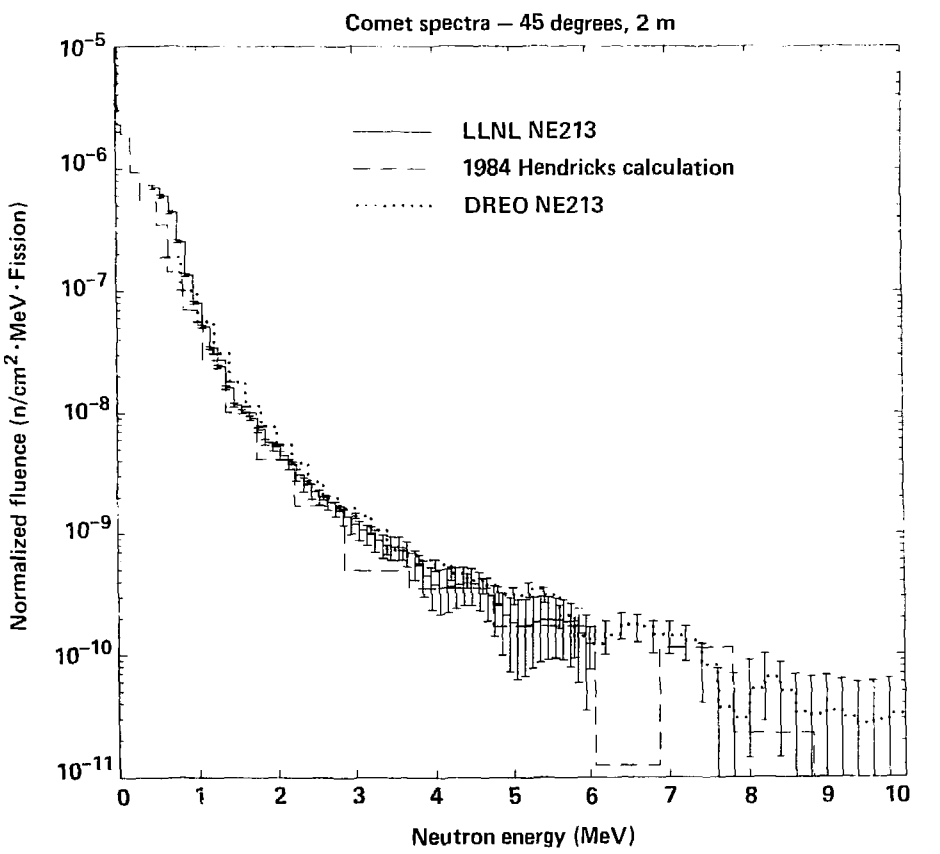
Griffith – Fig. 6



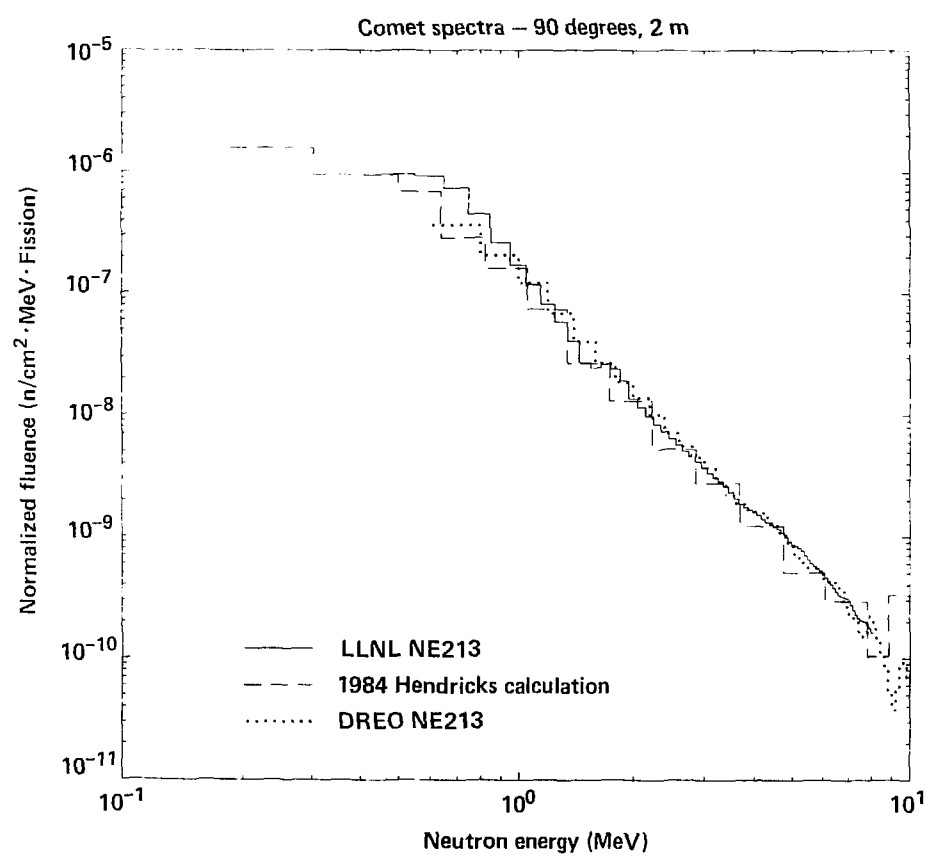
Griffith – Fig. 7



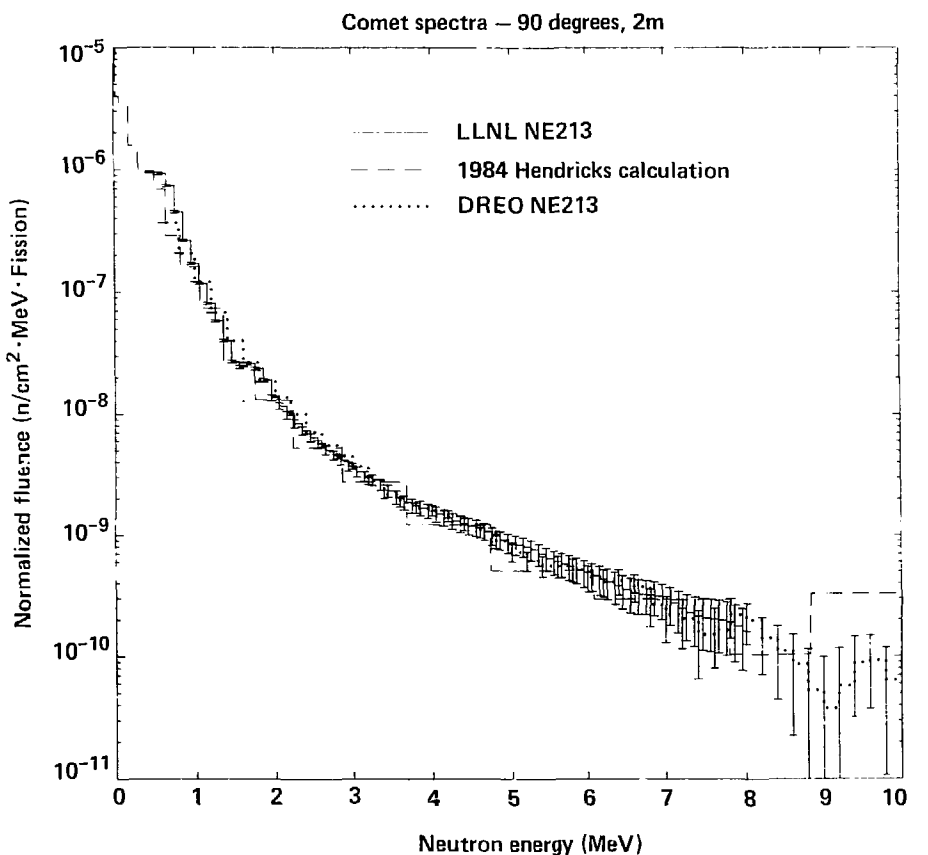
Griffith - Fig. 8



Griffith - Fig. 9



Griffith - Fig. 10



Griffith - Fig. 11